

Syn Schmitt · Michael Günther

Human leg impact: energy dissipation of wobbling masses

Received: 28 April 2010 / Accepted: 15 June 2010 / Published online: 6 July 2010
© Springer-Verlag 2010

Abstract In terrestrial locomotion, the soft-tissue masses of the body undergo damped oscillations following leg impacts with the ground. Appropriate biomechanical models, therefore, describe gross soft-tissue dynamics by “wobbling masses”. We calculated mechanical energy balances of shank and thigh wobbling masses of the stance leg for the first 90 ms after touch-down in human heel-toe running. Thereto, we re-visited a data set on wobbling mass kinematics which had formerly been gained non-invasively by acquiring the motion of grids of lines painted on the skin of the corresponding muscle masses with high-speed cameras. We found frequencies ranging from 3 Hz to 55 Hz and maximum wobbling mass excursions relative to the bone ranging from 3 mm to 4 cm for the centres of mass and from 2.2° to 11.4° for the rotations. The rotational energy balance is practically neutral (± 1 J). Usually, there is clearly more energy that is dissipated by wobbling mass movement in horizontal (thigh: <50 J) than in vertical direction (thigh: <15 J). There is less energy dissipated in the shank (horizontal: <10 J, vertical: <5 J). We argue that the energetic costs of separating significant wobbling masses from the skeleton may be over-compensated by avoiding metabolic costs of active impact reduction and by decreasing loads on passive skeletal structures, in particular when distal leg masses are functional, as in humans. Within reasonable biological limits, impacts are known to be even necessary for structural strengthening of bones. Beyond that, impacts might also be useful for stabilising locomotion, both by increasing basins of attraction and by providing simple mechanical signals for control.

Keywords Biomechanics · Locomotion · Human running · Soft tissue · Experimental analysis

1 Introduction

“Wobbling masses” were introduced, then using the one-off notation “wabbling”, by Denoth et al. [9] when simulating human sports activities with high accelerations. Earlier publications [25] followed an “effective

S. Schmitt (✉) · M. Günther
Institut für Sport- und Bewegungswissenschaft, Universität Stuttgart,
Allmandring 28, 70569 Stuttgart, Germany
E-mail: schmitt@inspo.uni-stuttgart.de
Tel: +49-711-685-60484
Fax: +49-711-685-50484

S. Schmitt
Cluster of Excellence for Simulation Technology, Universität Stuttgart,
Pfaffenwaldring 7a, 70569 Stuttgart, Germany

M. Günther
Institut für Sportwissenschaft, Lehrstuhl für Bewegungswissenschaft,
Friedrich-Schiller Universität, Seidelstraße 20, 07749 Jena, Germany

mass” concept by simulating the first 20 ms in impact situations of a three-segment rigid body model with the real shank mass halved. In refining this concept for numerical simulations of impacts in running, Nigg et al. [25] and Denoth et al. [8] assigned the ratio between vertical impact force peak and respective maximum acceleration of the tibia to the “effective mass” of just one segment. Gruber et al. [12] applied this concept to the estimation of knee joint loading during landings. They concluded that vertical impact force peaks not exceeding ten times body weight are well tolerable by the joints. With the introduction of “wobbling masses”, Denoth et al. [9] demonstrated that the omission of visco-elastic coupling of soft tissues in computer models for impacts inevitably results in joint loading beyond physiological tolerances. For example, the horizontal hip joint force exceeded the tolerance by more than sixfolds during impact. From later model calculations [13], it was concluded that neglecting the discrimination and dynamic coupling of bone and soft tissue in inverse dynamics would lead to a three- to fourfold overestimation of knee and hip joint torques and, as a consequence, of the corresponding muscle forces and joint loading.

Although there are stringent clues that the implementation of wobbling masses in models for impact situations improves results from inverse dynamics [1, 13, 15], some authors do still not seem to be convinced [2, 40]. Yet the wobbling mass concept has been consistently verified by the direct measurement of soft-tissue vibrations [36], by successfully reproducing the displacement of main leg muscle masses estimated in experiments [15], by a sensitivity analysis of wobbling mass influence on impact forces [29], by the influence of soft-tissue movement on ground reaction forces, joint torques, and joint forces in drop landings [30], and by predicting realistic mass distributions and impact force peaks [10]. The wobbling mass concept was applied to study human running [22, 26, 42, 43] and was used to formulate the hypothesis that muscle activity may be tuned to prevent soft-tissue resonance (“muscle tuning”) [5, 6, 34, 35, 37]. Moreover, three-dimensional human computer models including wobbling masses were established [20, 23, 32, 39, 41].

All in all, it seems that the wobbling mass concept has prevailed as a fundamental design concept for terrestrial locomotor systems bound to deal with impacts [3]. However, soft-tissue movement imposes energetic costs on the locomotor system [13, 26–28]. To our knowledge, these costs have not been detailed so far for those situations that have been in the focus of most of the previous wobbling mass analyses: human running. For this, we had already computed translational [15] and rotational [19] displacements of main soft-tissue masses in both main segments of the stance leg. The corresponding wobbling mass data set had been extracted from a high-speed analysis in which a grid of lines had been painted on the skin areas covering each the shank and the thigh. Here, we re-visited these running data in order to compute the mechanical energy balances of both wobbling masses during human leg impact, i.e. their potential costs.

2 Methods

2.1 Subject, experimental setup, data acquisition and processing

One male sports student (24 years, 67 kg, 1.78 m), who consented to the experiments, took part in this study. The experimental procedures were in accordance to the guidelines of the University of Jena Ethics Committee. Within five trials ($N = 5$) and during the first 90 ms following the instant of touch-down in heel-toe running, we measured the subject’s stance leg kinematics in the sagittal plane and the ground reaction forces (GRFs) underneath the foot, using high-speed cameras and a force plate, both recording simultaneously at 500 Hz. Details of the experimental setup, the data acquisition, and the processing of raw marker kinematics have been published elsewhere [15]. When compared to this, using a different low-pass filter constituted the only methodical deviation within this study. Instead of a zero-lag Butterworth filter [38] with a cut-off frequency 100 Hz, due to suppressed overshoot, a symmetric windowed-sinc filter with a Blackman window (7 samples) was applied to low-pass filter the raw kinematic and force data. The main methodical features from [15] are recapitulated in the subsequent paragraph.

To enable for the acquisition of wobbling mass kinematics of shank and thigh, the subject was prepared by painting a grid of black ink lines directly on the skin (Fig. 1a). Additionally, skin markers were attached to the ankle and the hip joint. Additionally, the horizontal position of the bony contour of the *tuberositas tibiae* was digitised manually to provide a measure of the horizontal knee coordinate not influenced by skin motion. Using both raw coordinates of the ankle marker, the horizontal contour coordinate (plus 7 cm offset), the horizontal hip marker coordinate low-pass filtered again with a zero-lag Butterworth (50 Hz cut-off frequency), and constant segment (bone) lengths of shank (42 cm) and thigh (44 cm), we computed the kinematics of the bony part of both segments. The positions of the centres of mass (COMs) of the bony parts and their angular orientations were calculated from these processed joint marker data. The whole segment masses and moments

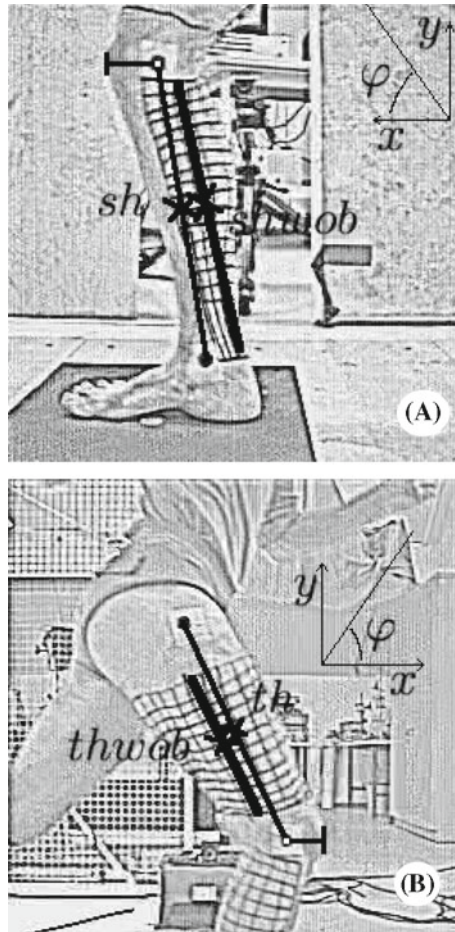


Fig. 1 Experimental preparation, kinematic analysis, and symbols for shank (a) and thigh (b) segments. Circles are joint markers attached to the skin (or computed from the patellar contour), a segment's wobbling mass is represented by the belonging *painted grid of black lines*. Thick X symbols labelled by sh, th and shwob, thwob, respectively, represent the centres of mass of bony and wobbling mass parts. A thin line connecting the distal and proximal circle illustrates the orientation of the segment's bony part, a thick line representing a linear best fit through all crossing points on a segmental grid illustrates the orientation of the segment's wobbling mass part. Top right sketches depicts the x, y-axes of the inertial system and the segmental angle φ

of inertia (MOIs) were estimated from anthropometric data based on literature [24], whereas the bony mass portions were estimated [15] as 50% (shank) and 66% (thigh). The coordinates $X_{k,\text{wob}}, Y_{k,\text{wob}}$ of the COM of a segment's (index k ; shank: $k = \text{sh}$; thigh: $k = \text{th}$) wobbling mass part were estimated from calculating the arithmetic mean of the coordinates of all digitised grid points on the respective segment (crossings of the lines painted on the skin above the muscle masses), assuming that each of the equally spaced grid points represented the motion of approximately the same portion of underlying soft-tissue mass.

2.2 Moment of inertia, coupling torques and forces, power and energy of the wobbling masses

In this study, as a further step which is yet in accordance with this approximate $X_{k,\text{wob}}, Y_{k,\text{wob}}$ estimation, we computed an angular orientation (in the inertial system: Fig. 1) $\varphi_{k,\text{wob}}$ of a segment's wobbling mass distribution by determining the linear regression line through the grid points, passing also through $X_{k,\text{wob}}, Y_{k,\text{wob}}$. Furthermore, we estimated the (time-dependent, time t) sagittal MOI of a segment's wobbling mass part $\theta_{k,\text{wob}}(t)$ by first calculating the sum

$$\tilde{\theta}_{k,\text{wob}}(t) = \sum_{i=1}^{P_k} r_{k,i}^2(t). \quad (1)$$

in proportion to the defining formula of the MOI, thereby tentatively assigning each the same mass 1 to a grid point. Here, i denotes the grid point on the segment k , whereas the total number of points taken into account is P_k and $r_{k,i}^2(t)$ symbolises the (time-dependent) squared distance from the estimated COM position of the wobbling mass ($X_{k,\text{wob}}, Y_{k,\text{wob}}$) to a grid point.

Knowing the approximate values of the whole (bone plus wobbling mass) segmental MOIs from anthropometric data and further assuming that the values of the MOIs of bone and wobbling mass parts scale in proportion with their relative mass percentages, we found the approximate anthropometric values $\theta_{\text{sh,wob}} = 0.02 \text{ kg m}^2$ and $\theta_{\text{th,wob}} = 0.08 \text{ kg m}^2$ for the wobbling mass MOIs of our subject. As the MOI values in fact fluctuate with time, we finally scaled the relative MOIs $\tilde{\theta}_{k,\text{wob}}(t)$ (Eq. 1) such that the absolute estimates $\theta_{k,\text{wob}}(t = 0)$ at the instant of touch-down ($t = 0$) equalled the anthropometric values given above.

The wobbling mass part of segment k can be modelled as one mechanical body that is attached to the bone by coupling force ($F_{k/x,\text{coup}}, F_{k/y,\text{coup}}$) and torque ($M_{k/z,\text{coup}}$) components. Its equations of motion (two translational and one rotational in the sagittal plane) are

$$F_{k/x,\text{coup}} = m_{k,\text{wob}} \cdot \ddot{X}_{k,\text{wob}}(t) \quad (2)$$

$$F_{k/y,\text{coup}} = m_{k,\text{wob}} \cdot (\ddot{Y}_{k,\text{wob}}(t) - g_y) \quad (3)$$

$$\begin{aligned} M_{k/z,\text{coup}} &= \dot{L}(t) \\ &= \theta_{k,\text{wob}}(t) \cdot \ddot{\varphi}_{k,\text{wob}}(t) + \dot{\theta}_{k,\text{wob}}(t) \cdot \dot{\varphi}_{k,\text{wob}}(t) \end{aligned} \quad (4)$$

whereat $L(t) = \theta_{k,\text{wob}}(t) \cdot \dot{\varphi}_{k,\text{wob}}(t)$ denotes the angular momentum of momentum of the wobbling mass part with respect to its COM and $g_y = -9.81 \text{ m/s}$ denotes the gravitational acceleration on earth. Thus, the current values of the coupling forces and torques can be directly estimated from measured wobbling mass kinematics. Consequently, the following sagittal contributions of a segment's wobbling mass motion to current mechanical power can be distinguished:

$$P_{k/x,\text{wob}}(t) = F_{k/x,\text{coup}}(t) \cdot \dot{X}_{k,\text{wob}}(t) \quad (5)$$

$$P_{k/y,\text{wob}}(t) = F_{k/y,\text{coup}}(t) \cdot \dot{Y}_{k,\text{wob}}(t) \quad (6)$$

$$P_{k/\varphi,\text{wob}}(t) = M_{k/z,\text{coup}}(t) \cdot \dot{\varphi}_{k,\text{wob}}(t). \quad (7)$$

Finally, integrating these contributions during the first 90 ms following the instant of touch-down provides the net mechanical energy balances of wobbling mass oscillations excited by leg impact:

$$\Delta E_{k/j,\text{wob}} = \int_{t=0}^{t=90 \text{ ms}} P_{k/j,\text{wob}} dt. \quad (8)$$

3 Results

Five trials of one subject in heel-toe running were analysed. The trial numbers in Tables 1, 2, 3 correspond to the row numbers of Table 2 already published [15]. All figures presented in the following are taken from one exemplary case (trial 1).

3.1 Forces, torques, kinematics, and moments of inertia

Table 1 summarises the maximum displacements of wobbling mass COMs of shank and thigh relative to the bone COMs in the bone coordinate system (transversal: $\Delta T_{k,f,\text{max}}$, longitudinal: $\Delta L_{k,f,\text{max}}$), and their maximum relative angular excursions ($\Delta \varphi_{k,f,\text{max}} = \varphi_{k,\text{wob}} - \varphi_k$) during the first 90 ms after the instant of touch-down. In order to determine the latter ones, the wobbling mass part was rotated by the mean difference in angular orientation with respect to the bony part. We distinguished high ($f = h$) and low ($f = l$) frequency oscillations. As a measure of leg impact intensity, the maximum impact GRF ($F_{x,\text{imp}}, F_{y,\text{imp}}$ for $t < 40 \text{ ms}$) are also reported. In all observed degrees of freedom (DOFs), be them transversal, longitudinal, or rotational, there is a high-frequency oscillation ranging from 15 to 55 Hz following the impact. Low-frequency oscillations occur at about 7 Hz (shank) and 3 Hz (thigh) in both longitudinal and transversal directions. They conform

Table 1 Heel-toe running: maximum GRF (impact: $F_{x,\text{imp}}$, $F_{y,\text{imp}}$ during first 40 ms after touch-down), maximum displacements between bone and wobbling mass COMs (with respect to the bone coordinate system; during first 90 ms after touch-down; transversal: $\Delta T_{k,f,\text{max}}$, longitudinal: $\Delta L_{k,f,\text{max}}$), and maximum relative angular excursions ($\Delta\varphi_{k,f,\text{max}} = \varphi_{k,\text{wob}} - \varphi_k$ during first 90 ms after touch-down) for high (h : \approx 15–55 Hz) and low frequency oscillations (l : \approx 4–7 Hz) of shank (sh, upper table) and thigh (th, lower table)

Trial	$F_{x,\text{imp}}$ (N)	$F_{y,\text{imp}}$ (N)	$\Delta T_{\text{sh},h,\text{max}}$ (m)	$\Delta T_{\text{sh},l,\text{max}}$ (m)	$\Delta L_{\text{sh},h,\text{max}}$ (m)	$\Delta L_{\text{sh},l,\text{max}}$ (m)	$\Delta\varphi_{\text{sh},h,\text{max}}$ (°)	$\Delta\varphi_{\text{sh},l,\text{max}}$ (°)
1	-330	2500	0.004	0.016	0.008	0.007	2.2	–
2	-470	2990	0.006	0.015	0.004	0.008	2.6	9.8
4	-410	2500	0.008	0.017	0.008	0.007	3.1	–
5	-390	1800	0.009	0.031	0.005	0.013	2.2	–
6	-380	1410	0.004	0.031	0.005	0.006	2.8	–
Trial	$F_{x,\text{imp}}$ (N)	$F_{y,\text{imp}}$ (N)	$\Delta T_{\text{th},h,\text{max}}$ (m)	$\Delta T_{\text{th},l,\text{max}}$ (m)	$\Delta L_{\text{th},h,\text{max}}$ (m)	$\Delta L_{\text{th},l,\text{max}}$ (m)	$\Delta\varphi_{\text{th},h,\text{max}}$ (°)	$\Delta\varphi_{\text{th},l,\text{max}}$ (°)
1	-330	2500	0.007	0.006	0.013	0.029	2.5	9.4
2	-470	2990	0.007	0.017	0.007	0.034	3.1	7.3
4	-410	2500	0.009	0.003	0.013	0.031	4.4	11.4
5	-390	1800	0.003	0.018	0.005	0.038	3.7	8.0
6	-380	1410	0.006	0.011	0.003	0.030	3.1	10.3

The trial number corresponds to the row number in Table 2 of Günther et al. [15]. The vertical impact force values $F_{y,\text{imp}}$ deviate slightly due to a different low-pass filter applied here

Table 2 Heel-toe running: maximum translational and rotational accelerations in the inertial system ($\ddot{x}_{k[\text{wob}],\text{max}}$, $\ddot{y}_{k[\text{wob}],\text{max}}$, $\ddot{\varphi}_{k[\text{wob}],\text{max}}$ during first 90 ms after touch-down) of bone and wobbling mass for shank (sh, upper table) and thigh (th, lower table)

Trial	$\ddot{x}_{\text{sh},\text{max}}$ (m/s ²)	$\ddot{y}_{\text{sh},\text{max}}$ (m/s ²)	$\ddot{\varphi}_{\text{sh},\text{max}}$ (°/s)	$\ddot{x}_{\text{sh,wob},\text{max}}$ (m/s ²)	$\ddot{y}_{\text{sh,wob},\text{max}}$ (m/s ²)	$\ddot{\varphi}_{\text{sh,wob},\text{max}}$ (°/s)
1	-81	209	-33900	-71	265	-53700
2	-110	194	-35000	-70	240	-57600
4	-204	156	-35400	-88	270	-66400
5	-133	136	-23500	-92	144	-32200
6	-139	103	-38100	-67	122	-38100
Trial	$\ddot{x}_{\text{th},\text{max}}$ (m/s ²)	$\ddot{y}_{\text{th},\text{max}}$ (m/s ²)	$\ddot{\varphi}_{\text{th},\text{max}}$ (°/s)	$\ddot{x}_{\text{th,wob},\text{max}}$ (m/s ²)	$\ddot{y}_{\text{th,wob},\text{max}}$ (m/s ²)	$\ddot{\varphi}_{\text{th,wob},\text{max}}$ (°/s)
1	-69	145	29400	87	143	-48100
2	-59	172	22400	126	175	-48000
4	132	148	39400	-76	76	-62700
5	86	104	26300	-71	-55	-40200
6	-125	75	17700	-76	39	41000

Table 3 Heel-toe running: energy balances ($\Delta E_{k/x,\text{wob}}$, $\Delta E_{k/y,\text{wob}}$, $\Delta E_{k/\varphi,\text{wob}}$ during first 90 ms after touch-down; $\Delta E_{k/j,\text{wob}} < 0$ means energy loss) of shank (sh) and thigh (th) wobbling masses

Trial	$\Delta E_{\text{sh}/x,\text{wob}}$ (J)	$\Delta E_{\text{sh}/y,\text{wob}}$ (J)	$\Delta E_{\text{sh}/\varphi,\text{wob}}$ (J)	$\Delta E_{\text{th}/x,\text{wob}}$ (J)	$\Delta E_{\text{th}/y,\text{wob}}$ (J)	$\Delta E_{\text{th}/\varphi,\text{wob}}$ (J)
1	-4.9	-4.4	0.1	-18.2	-13.4	-0.2
2	-4.1	-3.5	0.0	-11.8	-13.5	0.0
4	-9.0	-2.6	-0.2	-37.1	-6.5	-0.9
5	-9.0	-1.1	-0.2	-38.9	-3.3	-0.1
6	-9.5	-1.4	-0.2	-46.9	-4.4	0.5

to the typical periods of the segment rotations during the complete stance phase. Due to the limited display window of the camera, we could specify the angular low-frequency content of the shank segment within just one trial. Our data are well in accordance to literature. One study [28] found low-frequency oscillations around 3 Hz and high-frequency oscillations in the range 11–20 Hz. Karlsson and Tranberg [18] published skin marker displacements of 4–8 mm in transversal and 1–4 mm in longitudinal directions, and resonant frequencies of 17–51 Hz. Others [36] ascertained skin motions of 8–80 Hz for tangential and 8–58 Hz for normal vibrations. Experimentally, Pain and Challis [30] determined very similar magnitudes (shank: 18 mm, thigh: 32 mm) and frequency contents (shank: 14–50 Hz, thigh: 14–18 Hz) of soft-tissue motion.

Figure 2a shows the x - and y -accelerations of the bony parts of the segments at the knee and hip joint, computed by our analysis of ankle, knee, and hip marker kinematics. The corresponding accelerations of the wobbling mass parts are plotted in Fig. 2b (x), c (y), and d (φ). For the five trials analysed, the maximum translational and rotational accelerations (\ddot{x}_k,max , \ddot{y}_k,max , $\ddot{\varphi}_k,\text{max}$) of bone and wobbling mass parts are listed in

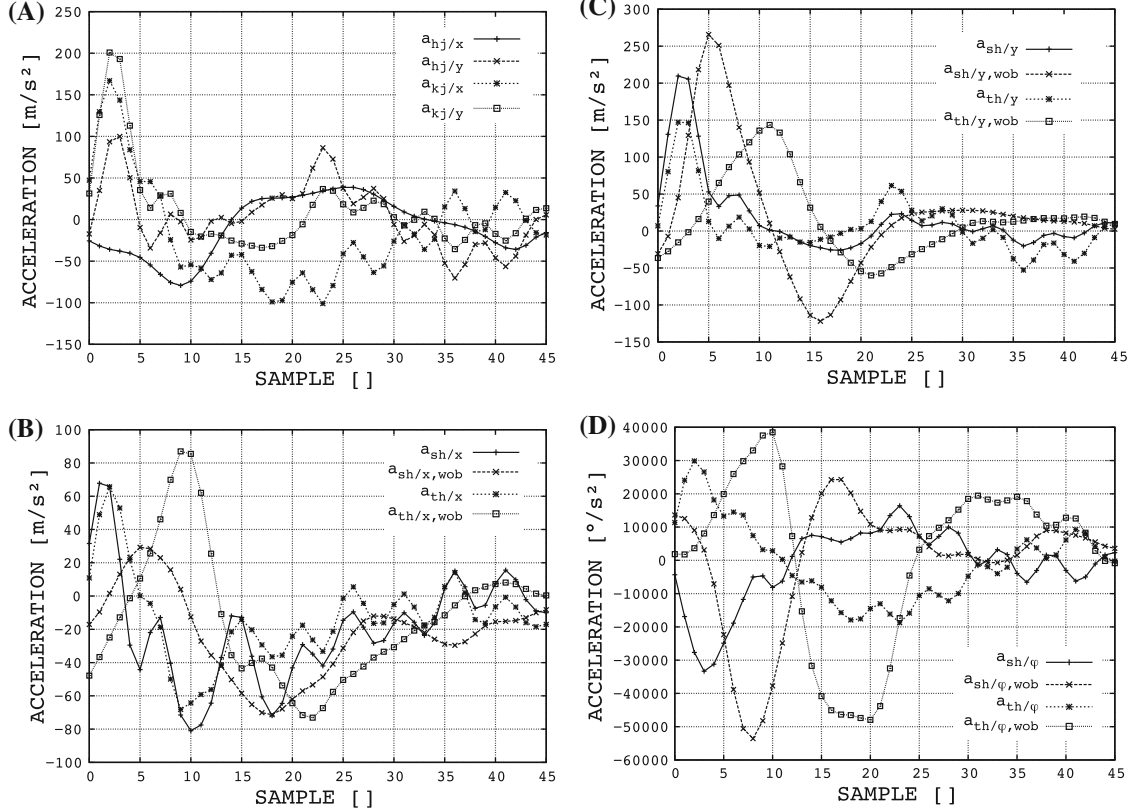


Fig. 2 Trial 1 (first 90 ms after touch-down in heel-toe running): **(a)** Acceleration of the bone at the knee ($a_{kj/x}$, $a_{kj/y}$) and hip ($a_{hj/x}$, $a_{hj/y}$) joint computed from the kinematics of the *circle markers* attached to the skin at knee and hip. Translational acceleration in x - **(b)** and y -direction **(c)**, and rotational acceleration in φ -direction **(d)** of shank (sh) and thigh (th) of both bony (k/j) and wobbling mass (k/j,wob) parts

Table 2. The data are well in accordance to literature of maximum tibia acceleration (<10 g) for shod heel-toe running at 4.7 m/s [21]. Maximum acceleration values double as high in our data reflect our barefoot condition, running at the same speed.

Figure 3 illustrates that the computed MOIs of the wobbling mass parts fluctuate slightly (shank: <13%, thigh: <5%). The maximum coupling forces and torques in the inertial system for the shank segment (Fig. 4a) are $F_{k/x,\text{coup}} = -111 \text{ N}$, $F_{k/y,\text{coup}} = 409 \text{ N}$, and $M_{k/z,\text{coup}} = -16 \text{ Nm}$. For the thigh segment we get $F_{k/x,\text{coup}} = 390 \text{ N}$, $F_{k/y,\text{coup}} = 684 \text{ N}$, and $M_{k/z,\text{coup}} = -57 \text{ Nm}$ (Fig. 4b). Note that the term $\dot{\theta}_{k,\text{wob}} \cdot \dot{\varphi}_{k,\text{wob}}$ (last row in Eq. 2) makes always less than 10% of maximum $M_{k/z,\text{coup}}$, i.e. less than 1.5 Nm in the shank and less than 3.5 Nm in the thigh.

3.2 Energy

The 90 ms balances (Eq. 8) of the five trials are listed in Table 3. Negative values mean energy dissipation (loss). For our exemplary trial 1, Fig. 5a (shank) and b (thigh) depict the time courses of wobbling mass energy balances $\Delta E_{k/j,\text{wob}}$ for the first 90 ms after touch-down in x -, y -, and φ -direction. In this, the following chronology can be observed. First, until ≈ 20 ms, energy is dissipated by vertical coupling in both segments. In both segments, this energy dissipation concurs to an energy release from horizontal coupling. Thereby, horizontal release is as high as vertical dissipation in the thigh, but just about a fourth of vertical dissipation in the shank. Second, starting from 20 to 50 ms (shank) and from 25 to 60 ms (thigh) energy is dissipated by horizontal wobbling mass coupling. The corresponding rotational energies show a maximum exactly at the beginning of this second phase, i.e. intermittently the coupling even increases the rotational (kinetic) energy of the respective wobbling mass. However, in total the rotational coupling does virtually not contribute to energy dissipation after touch-down.

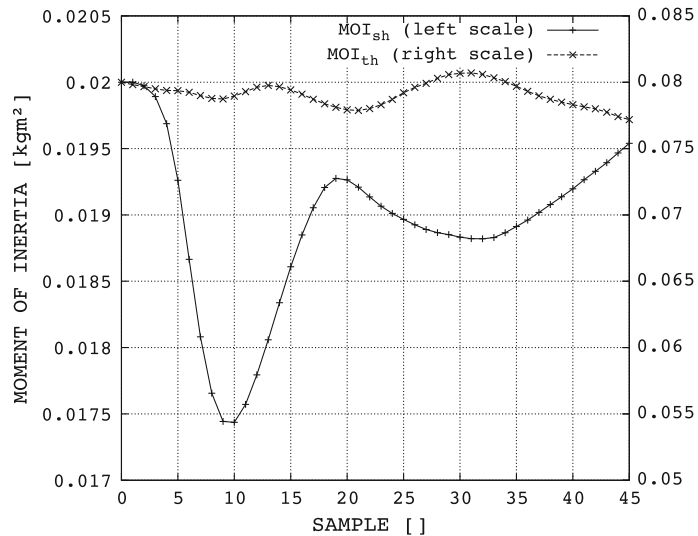


Fig. 3 Trial 1: Sagittal moment of inertia of shank (*left scale*) and thigh (*right scale*) for the first 90 ms after touch-down in heel-toe running

4 Discussion

4.1 Validity of the method

We have found that the net energy loss due to wobbling masses in the stance leg ranges from 30 to 60 J per stance phase. These values represent a minimum guess. In the first instance, there is uncertainty in how the muscle mass displacements are transferred to skin motion. At least, a former study [15] demonstrated that our estimation of the centres of wobbling masses consistently maps the acceleration signals predicted by a direct dynamic simulation of a reduced model [13], even though both approaches were completely independent. Furthermore, it remains open to which amount other phenomena cause further dissipation. For example, neither torsion around the longitudinal axis, nor medio-lateral displacement or twist, nor excitation of any even mode are mapped by our macroscopic coordinates ($\varphi_{k,i}, X_{k,i}, Y_{k,i}$). In an optimised approach, a three-dimensional analysis of wobbling mass motion would be used to validate a biomechanical model predicting muscle mass dynamics. Then, beyond pure mechanics, a validated model would even allow for the calculation of metabolic contributions to energy dissipation. If, moreover, an energy balance of whole-body movement were in the focus of interest, beside determining all joint torques, the motion of trunk wobbling masses (muscles, blood, viscera) would expectedly have to be factored in. With this, however, it becomes obvious what a tricky task a consistent calculation of energy balances can be. In as much as movement of wobbling masses, e.g. in the leg, is often mostly due to muscles of which the forces certainly dominate the joint torques. To say it differently, part of the coupling forces should be contractile muscle forces; however, their exact relation is currently unknown. It is all up to an integrated modelling of muscle contraction, visco-elastic contact forces between tissue compartments, and inertia properties of muscle masses.

4.2 Energy balances during ground contact in running

Recently, Grimmer et al. [11] made a considerable step to approach a global mechanical energy balance in human running. During the complete stance phase, they calculated a mean maximum elastic energy exchange of about ≈ 100 J between all storages of potential energy internal to the body (the virtual leg) and the kinetic translational energy of the whole-body COM in the sagittal plane. Thus, they probably quantified the main contribution to a mechanical energy balance of whole-body movement. Moreover, they found that the virtual leg dissipates on average 8–27 J in level running, i.e. up to about one fourth of the maximum energy stored in the virtual leg.

Also during level running at about 5 m/s, Günther et al. [14] calculated the local (joint) mechanical energy balances of the stance leg. They found that the three joints (ankle 24 J, knee –3 J, hip 37 J) release about 50–60 J

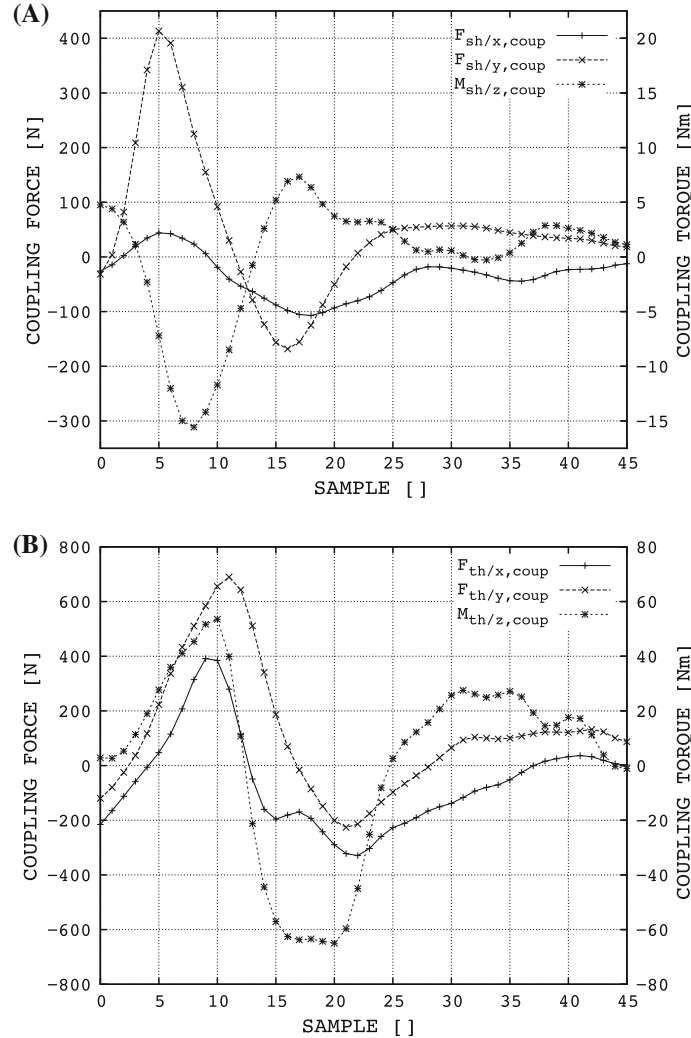


Fig. 4 Trial 1: Coupling forces (left scale) and torque (right scale) ($F_{k/x,coup}$, $F_{k/y,coup}$, $M_{k/z,coup}$; see Eq. 2) between bone and wobbling mass parts of the shank (a) and thigh (b) segment in the inertial system for the first 90 ms after touch-down in heel-toe running

on average and in total during the stance phase. Thus, net joint energy release in all three leg joints would be suitable to compensate about for the losses due to wobbling mass motion. When compared to the (global translational) virtual leg balance, the (local) wobbling mass loss is about double as high as leg dissipation and about half of the maximum energy stored in the leg.

4.3 What is gained from wobbling masses?

Compared to other species, humans have large distal leg masses. Therefore, avoiding impacts by decelerating these masses actively during locomotion would involve both enormous energetic costs and control effort [3]. Additionally, it has been shown that a non-vanishing touch-down velocity of the foot relative to the ground, inevitably inducing impacts, enhances movement stability (mechanism of leg retraction: [31]) and, beyond, the corresponding basin of attraction [4]. Furthermore, the shock wave induced by the leg impact might represent simply coded information useful for movement self-stabilisation [11]. Finally, impacts seem to be essential, below the limits of biologically tolerable magnitudes, for maintaining the skeletal structure [7, 16, 17, 33]. When exceeding these limits, high impacts reduce lifetime of biological material as bones, cartilage, and muscle-tendon complexes [3]. Wobbling masses are a means to reduce high impacts by suspending

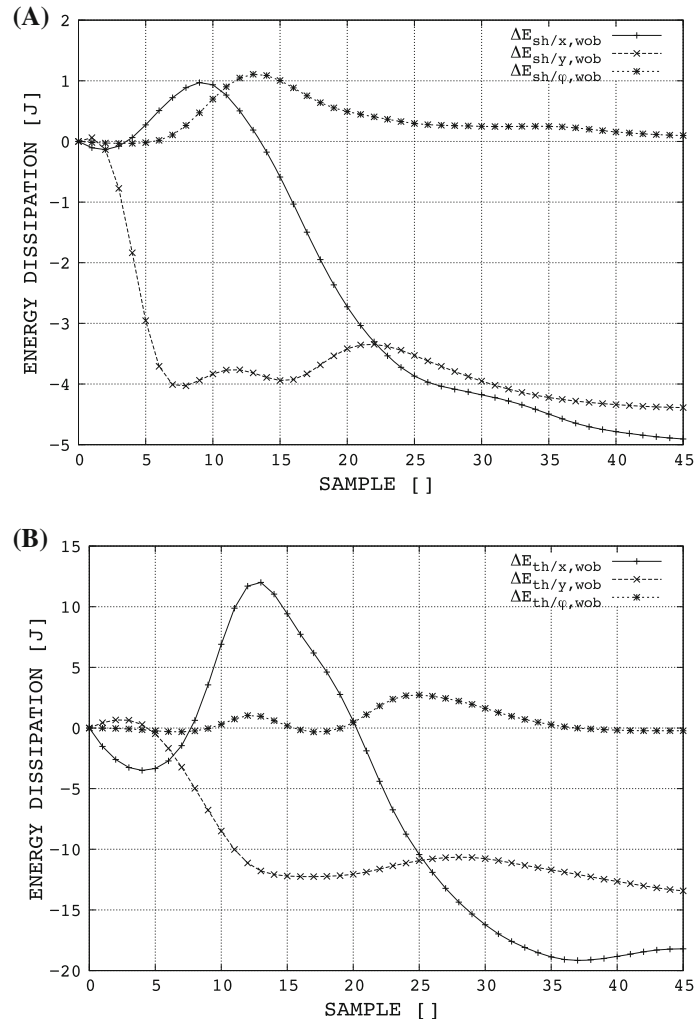


Fig. 5 Trial 1: Mechanical energy balance of the wobbling mass part of the shank (a) and thigh (b) segment in the inertial system for the first 90 ms after touch-down in heel-toe running

the muscles visco-elastically to the skeleton [15]. The suspension forces can obviously be tuned to different loading conditions [5, 6, 34, 35, 37].

All in all, assuming good reasons for the existence of relatively large distal leg masses, e.g. evolutionary constraints like bipedal upright stance or motor adaptability and versatility, the costs of wobbling mass motion are probably well over-compensated by the aforementioned benefits of tolerating moderate impacts. Thereby, the actuators of biological locomotor systems are evidently designed to withstand impacts. The ingenuity of natural design expresses itself in yielding actuators, the muscles, that both incorporate the wobbling mass functionality and refined contractile properties.

Acknowledgments SS and MG were kindly supported by “Deutsche Forschungsgemeinschaft” (DFG), SS within the Cluster of Excellence in Simulation Technology (Universität Stuttgart: EXC310/1) and MG by grant MU1766/1-3.

Conflict of interest The authors declare that they have no conflict of interest.

References

1. Alonso, F.J., Del Castillo, J.M., Pintado, P.: Motion data processing and wobbling mass modelling in the inverse dynamics of skeletal models. *Mech. Mach. Theory* **42**(9), 1153–1169 (2007)
2. Bisseling, R.W., Hof, A.L.: Handling of impact forces in inverse dynamics. *J. Biomech.* **39**(13), 2438–2444 (2006)

3. Blickhan, R., Seyfarth, A., Geyer, H., Grimmer, S., Wagner, H., Günther, M.: Intelligence by mechanics. *Philos. Trans. Ser. A Math. Phys. Eng. Sci.* **365**(1850), 199–220 (2007)
4. Blum, Y., Lipfert, S.W., Rummel, J., Seyfarth, A.: Swing leg control in human running. *Bioinspir. Biomim.* (2010) [Epub ahead of print]
5. Boyer, K.A., Nigg, B.M.: Soft tissue vibrations within one soft tissue compartment. *J. Biomech.* **39**(4), 645–651 (2006)
6. Boyer, K.A., Nigg, B.M.: Quantification of the input signal for soft tissue vibration during running. *J. Biomech.* **40**(8), 1877–1880 (2007)
7. Davis, B.L., Cavanagh, P.R., Sommer, H.J. III., Wu, G.: Ground reaction forces during locomotion in simulated microgravity. *Aviat. Space Environ. Med.* **67**(3), 235–242 (1996)
8. Denoth, J.: The dynamic behaviour of a three link model of the human body during impact with the ground. In: Winter, D.A., Norman, R.W., Wells, R.P., Hayes, K.C., Patla, A.E. (eds.) *Biomechanics IX-A*, Volume 5B of International Series on Biomechanics, pp. 102–106. Human Kinetics, Champaign (1985)
9. Denoth, J., Gruber, K., Ruder, H., Keppler, M.: Forces and torques during sports activities with high accelerations. In: Perren, S.M., Schneider, E. (eds.) *Biomechanics: Current interdisciplinary research*, International Series on Biomechanics, pp. 663–668. Martinus Nijhoff, Amsterdam (1985)
10. Gittoes, M.J.R., Brewin, M.A., Kerwin, D.G.: Soft tissue contributions to impact forces simulated using a four-segment wobbling mass model of forefoot-heel landings. *Hum. Mov. Sci.* **25**(6), 775–787 (2006)
11. Grimmer, S., Ernst, M., Günther, M., Blickhan, R.: Running on uneven ground: leg adjustment to vertical steps and self-stability. *J. Exp. Biol.* **211**(Pt 18), 2989–3000 (2008)
12. Gruber, K., Denoth, J., Stuessi, E., Ruder, H.: The wobbling mass model. In: Jonsson, B. (ed.) *Biomechanics X-B*, Volume 6B of International Series on Biomechanics, pp. 1095–1099. Human Kinetics, Champaign (1987)
13. Gruber, K., Ruder, H., Denoth, J., Schneider, K.: A comparative study of impact dynamics: wobbling mass model versus rigid body models. *J. Biomech.* **31**(5), 439–444 (1998)
14. Günther, M., Blickhan, R.: Joint stiffness of the ankle and the knee in running. *J. Biomech.* **35**(11), 1459–1474 (2002)
15. Günther, M., Sholukha, V.A., Keßler, D., Wank, V., Blickhan, R.: Dealing with skin motion and wobbling masses in inverse dynamics. *J. Mech. Med. Biol.* **3**(3/4), 309–335 (2003)
16. Järvinen, T.L., Kannus, P., Sievanen, H., Jolma, P., Heinonen, A., Järvinen, M.: Randomized controlled study of effects of sudden impact loading on rat femur. *J. Bone Miner. Res.* **13**(9), 1475–1482 (1998)
17. Jorgensen, L., Crabtree, N.J., Reeve, J., Jacobsen, B.K.: Ambulatory level and asymmetrical weight bearing after stroke affects bone loss in the upper and lower part of the femoral neck differently: bone adaptation after decreased mechanical loading. *Bone* **27**(5), 701–707 (2000)
18. Karlsson, D., Tranberg, R.: On skin movement artefact-resonant frequencies of skin markers attached to the leg. *Hum. Mov. Sci.* **18**(5), 627–635 (1999)
19. Keppler, V., Günther, M.: Visualization and quantification of wobbling mass motion—a direct non-invasive method. *J. Biomech.* **39**(1), 53 (2006)
20. Kraus, C., Bock, H.G., Mutzschler, H.: Parameter estimation for biomechanical models based on a special form of natural coordinates. *Multibody Syst. Dyn.* **13**(1), 101–111 (2005)
21. Lafontaine, M.A.: Three-dimensional acceleration of the tibia during walking and running. *J. Biomech.* **24**(10), 877–886 (1991)
22. Liu, W., Nigg, B.M.: A mechanical model to determine the influence of masses and mass distribution on the impact force during running. *J. Biomech.* **33**(2), 219–224 (2000)
23. Mills, C., Pain, M.T.G., Yeadon, M.R.: The influence of simulation model complexity on the estimation of internal loading in gymnastics landings. *J. Biomech.* **41**(3), 620–628 (2008)
24. NASA Reference Publication. Anthropometric Source Book. Technical Report 1024, I-III, NASA Scientific and Technical Information Office, Springfield (1978)
25. Nigg, B.M., Denoth, J.: Belastung des menschlichen Bewegungsapparates aus der Sicht der Biomechanik. In: Nigg, B.M., Denoth, J. (eds.) *Sportplatzbeläge*, pp. 33–77. Juris, Zürich (1980)
26. Nigg, B.M., Liu, W.: The effect of muscle stiffness and damping on simulated impact force peaks during running. *J. Biomech.* **32**(8), 849–856 (1999)
27. Pain, M.T.G., Challis, J.H.: The role of the heel pad and shank soft tissue during impacts: a further resolution of a paradox. *J. Biomech.* **34**(3), 327–333 (2001)
28. Pain, M.T.G., Challis, J.H.: Soft tissue motion during impacts: their potential contributions to energy dissipation. *J. Appl. Biomed.* **18**(3), 231–241 (2002)
29. Pain, M.T.G., Challis, J.H.: Wobbling mass influence on impact ground reaction forces: a simulation model sensitivity analysis. *J. Appl. Biomed.* **20**(3), 309–316 (2004)
30. Pain, M.T.G., Challis, J.H.: The influence of soft tissue movement on ground reaction forces, joint torques and joint reaction forces in drop landings. *J. Biomech.* **39**(1), 119–124 (2006)
31. Seyfarth, A., Geyer, H., Herr, H.: Swing-leg retraction: a simple control model for stable running. *J. Exp. Biol.* **206**(15), 2547–2555 (2003)
32. Stelzer, M., Stryk, O.: Efficient forward dynamics simulation and optimization of human body dynamics. *Zeitschrift für Angewandte Mathematik Und Mechanik* **86**(10), 828–840 (2006)
33. Taaffe, D.R., Robinson, T.L., Snow, C.M., Marcus, R.: High-impact exercise promotes bone gain in well-trained female athletes. *J. Bone Miner. Res.* **12**(2), 255–260 (1997)
34. Wakeling, J.M., Liphardt, A., Nigg, B.M.: Muscle activity reduces soft-tissue resonance at heel-strike during walking. *J. Biomed.* **36**(12), 1761–1769 (2003)
35. Wakeling, J.M., Nigg, B.M.: Modification of soft tissue vibrations in the leg by muscular activity. *J. Appl. Physiol.* **90**(2), 412–420 (2001)
36. Wakeling, J.M., Nigg, B.M.: Soft-tissue vibrations in the quadriceps measured with skin mounted transducers. *J. Biomed.* **34**(4), 539–543 (2001)

37. Wakeling, J.M., Nigg, B.M., Rozitis, A.I.: Muscle activity damps the soft tissue resonance that occurs in response to pulsed and continuous vibrations. *J. Appl. Physiol.* **93**(3), 1093–1103 (2002)
38. Winter, D.A.: Biomechanics and Motor Control of Movement. 2nd edn. Wiley, New York (1990)
39. Wojtyra, M.: Multibody simulation model of human walking. *Mech. Based Des. Struct. Mach.* **31**(3), 357–379 (2003)
40. Yeow, C.H., Lee, P.V.S., Goh, J.C.H.: Effect of landing height on frontal plane kinematics, kinetics and energy dissipation at lower extremity joints. *J. Biomech.* **42**(12), 1967–1973 (2009)
41. Yue, Z., Mester, J.: A model analysis of internal loads, energetics, and effects of wobbling mass during the whole-body vibration. *J. Biomech.* **35**(5), 639–647 (2002)
42. Zadpoor, A.A., Nikooyan, A.A.: A mechanical model to determine the influence of masses and mass distribution on the impact force during running—a discussion. *J. Biomech.* **39**(2), 388–390 (2006)
43. Zadpoor, A.A., Nikooyan, A.A., Arshi, A.R.: A model-based parametric study of impact force during running. *J. Biomech.* **40**(9), 2012–2021 (2007)